

Fluorescence spectroscopy of graphene quantum dots: temperature effect at different excitation wavelengths

This content has been downloaded from IOPscience. Please scroll down to see the full text.

2014 Nanotechnology 25 435703

(<http://iopscience.iop.org/0957-4484/25/43/435703>)

View [the table of contents for this issue](#), or go to the [journal homepage](#) for more

Download details:

IP Address: 59.172.176.35

This content was downloaded on 08/04/2015 at 09:42

Please note that [terms and conditions apply](#).

Fluorescence spectroscopy of graphene quantum dots: temperature effect at different excitation wavelengths

Changzheng Li and Yanan Yue

School of Power and Mechanical Engineering, Wuhan University, Wuhan, Hubei 430072, People's Republic of China

E-mail: yyue@whu.edu.cn

Received 11 June 2014, revised 25 August 2014

Accepted for publication 8 September 2014

Published 9 October 2014

Abstract

This paper reports a comprehensive study of temperature dependence of fluorescence spectroscopy of graphene quantum dots at different excitation wavelengths. Very significant (more than 50%) and similar decrease of normalized spectrum intensity is observed within temperature range less than 80 °C for excitation wavelengths of 310 nm, 340 nm and 365 nm. Besides, the temperature dependence of the red-shift of spectrum peak shows different wavelength dependence characteristic with coefficient as high as 0.062 nm K⁻¹ for the same temperature range, which gives us a hint about selecting the right excitation wavelength by compromising the excitation efficiency for fluorescence intensity and the temperature coefficient for peak shift in thermal applications. Temperature dependence of peak width is in a weakly linear relationship with a coefficient of 0.026 nm K⁻¹. Regarding the excellent stability and reversibility during thermal measurement, graphene quantum dot is a good candidate for the implementation in the nanoscale thermometry, especially in the bio-thermal field considering its superior biocompatibility and low cytotoxicity.

Keywords: graphene quantum dots, fluorescence spectroscopy, temperature

(Some figures may appear in colour only in the online journal)

1. Introduction

Graphene, a monolayer or few layers of sp²-bonded carbon atoms, have attracted much attention for its exceptional properties, such as high carrier mobility and superior mechanical/thermal properties [1]. As small fragments of graphene (typically with size below 20 nm in diameter), graphene quantum dots (GQDs) receive significant interests due to the size-dependent band gap from quantum confinement and edge effects [2, 3]. They can be used in a wide range of potential applications crossing bio-imaging [4–6], energy conversion [7–11], and sensors [12]. Like other quantum dots, the photoluminescence (PL) spectrum of GQDs is closely related to the size and shape [3], but the bandwidth is much wider [13]. For quantum dots, different synthetic processes produce samples with different functional groups, which could affect fluorescence spectroscopy (e.g. red-shifted

emissions with a high surface oxidation degree) [14]. To date, tons of works have been focused on the effect of synthesis process and the modification of the particles on its fluorescence spectroscopy of GQDs [8, 10, 13, 15].

Thermal equilibrium state of quantum dots is another factor which significantly impacts its quantum efficiency in the photon excitation and emission. This characteristic can be employed in fluorescence thermometry for nanoscale thermal probing/imaging [16]. In the past, the temperature dependence of fluorescence spectroscopy of other semiconductor quantum dots has been studied. For example, Dai *et al* [17] studied the thermal relaxation of the PL in InAs/GaAs quantum dots and found that the linewidth first decreases and then increases with increasing temperature. Glen *et al* [18] reported a phenomenon that the steady-state PL intensity of cadmium selenide quantum dots decreases with temperature from 100 to 315 K. The peak position (frequency) of the PL

spectrum shifts by 20 nm over the same temperature range. Salman *et al* [19] investigated the temperature effects on the absorption and fluorescence spectrum of colloidal CdSe nanocrystals, they found that the emission spectrum behaved very differently for different shapes. Recently, Li *et al* [20] demonstrated CdSe quantum dots could be used for non-contact, local temperature measurements. They successfully evaluated the temperature profile of a MEMs microheater under different voltages by using the CdSe QDs. In another work, Gu *et al* [21] used PbSe QDs as temperature sensor to measure the temperature profile of GaN LED chips.

As a novel material, QDs have a great potential being used in a wide range of applications for its fluorescence excitations. Temperature is an important factor affecting its performance while not much attention has been focused on it. It remains as a question that how and to what extent will temperature affect the fluorescence spectroscopy of QDs. In nanoscale thermal probing field, there is an obstacle to find a stable thermometer for phonon transport study. In this work, we will report a preliminary study of temperature dependence of fluorescence spectroscopy of QDs and discuss different features of using QDs as thermometer in a wide range of applications.

2. Experimental details

2.1. Sample preparation and characterization

GQDs sample was purchased from ACS Material company and synthesized by bottom-up method. The bottom-up method refers to the synthesis of graphene moieties with aromatic structures such as fullerenes, the properties of which can be excellently controlled [22]. GQDs have a well-distributed size of 15 nm and thickness of 0.5–2 nm as indicated by the manufacturer. Sample is stably immersed in water solution with a concentration of 1 mg mL⁻¹. To specify the sample's size, the AFM image of the GQDs was taken on the platform of SHIMADZU SPM-9500J3. As shown in figure 1, the average thickness of three GQDs selected randomly is about 0.71 nm, agreeing well with the sample description provided by the supplier.

2.2. Fluorescence spectroscopy experiment

Fluorescence experiment is performed on a Horiba Jobin Yvon Fluorolog-3 fluorescence spectrometer. As shown in figure 2, the spectrometer is built with a 450 W xenon CW lamp. Adjustable excitation wavelength from 200 to 700 nm can be obtained through an excitation monochromator. The sample is fixed in a temperature controlling compartment and the temperature of sample can be precisely controlled with accuracy 0.01 °C. All-reflective optics in the compartment reflect all signals emitted from the sample, ensuring that the collected signal does not affected by the focal level of the light. An emission monochromator is used for collecting emitted photon with wavelength range from 300 to 1000 nm. In the experiment, the slit width and the integration time were

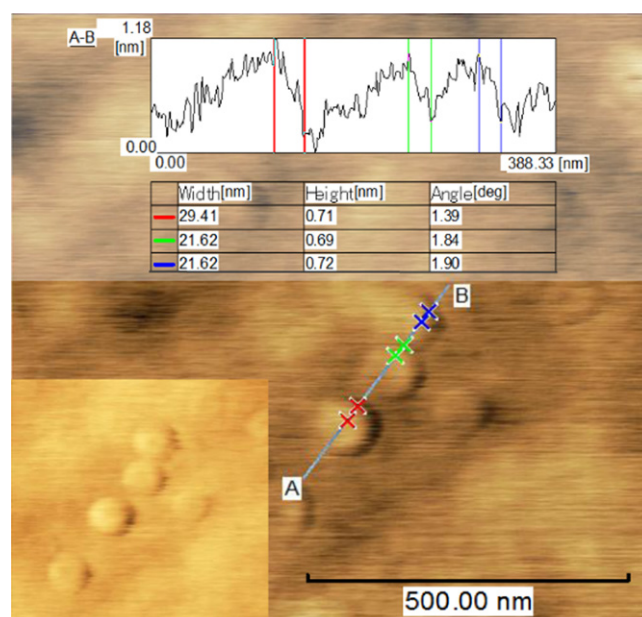


Figure 1. AFM image of our sample shows that the average thickness of three GQDs selected randomly is about 0.71 nm. The magnified image in lower-left shows the GQDs particles have a well-size distribution.

set to 5 nm and 0.1 s for ensuring a strong signal. Since GQDs are immersed in the water to keep stable, the fluorescence measurement is conducted at temperature below 100 °C (from 5 to 80 °C), respectively. Before each signal collection, the sample is maintained for 10 min at each temperature to ensure that the sample's temperature is stable. The spectrum is recorded three times at each temperature for averaging.

3. Results and discussions

3.1. Fluorescence spectrum at different excitation wavelengths

Figure 3(a) shows the absorption characteristics of GQDs. There are two peaks located at about 265 nm and 310 nm, corresponding to two absorption bands of our sample, which is similar to the result reported by Pan *et al* [13]. The inserts are sample images under visible light and UV beam respectively. The excellent emission of blue-luminescence under UV beam reveals that GQDs is very effective for fluorescence excitation. Figure 3(b) shows the fluorescence spectrum of GQDs at different excitation wavelengths at room temperature. Broad PL bandwidth can be found when the sample is excited under different wavelengths. The strongest signal at 425 nm is observed with excitation wavelength of 310 nm which falls into the absorption band of GQDs. In addition, shorter wavelength with higher photon energy is more effective for photon excitation. Thus, it is desirable to use shorter wavelength light source for fluorescence experiment. The PL peaks shifts from 425 to 458 nm and the intensity decreases as excitation wavelength is varied from 310 to 365 nm, which is very similar with other QDs [10, 13–15], and is caused by the emissive traps, electronic conjugate

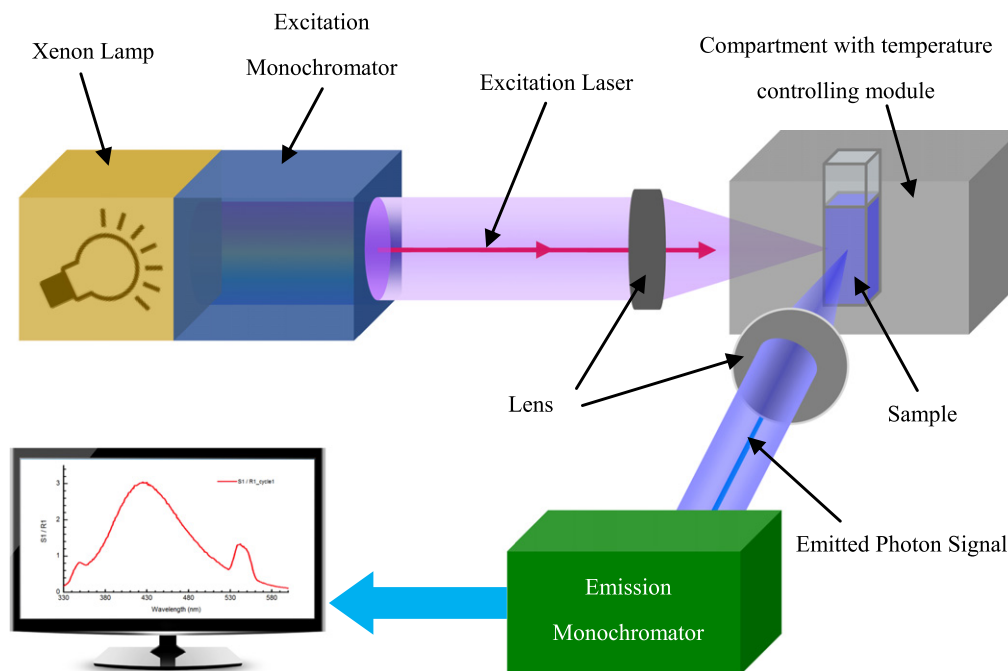


Figure 2. Schematic diagram of the fluorescence experiment (not to scale). A 450 W xenon CW lamp is used as the light source. Adjustable excitation wavelength can be obtained through an excitation monochromator. In the experiment, the sample is fixed in a compartment, which is automated temperature-control with the accuracy 0.01 °C. The setup of all-reflective optics inside the compartment (not shown in this figure) ensures that collected fluorescence signal is not affected by the focal level of the light.

structures, free zigzag sites, and the surface states of quantum dots [5, 10, 11, 15, 23].

It's observed that there are two sub-peaks on both sides of the prominent peak in the PL spectrum of the QDs, which are caused by the Raman scattering of water. To separate the QDs' signal from overall spectrum, we first measure the emission spectrum of distilled water, and then subtract it from the overall spectrum. Figure 3(b) shows the water emission spectrum at different excitation wavelengths and different temperatures. It is found that there is little temperature dependence for the Raman emission of water at the same excitation wavelength, which is good for our analysis by two means: first, the temperature dependence of QDs can be solely studied without considering the effect of water; second, the emitted signal is not affected by the focusing problem in fluorescence measurement.

3.2. Temperature dependence of fluorescence spectrum

Figure 4 shows the temperature dependence of fluorescence spectrum of QDs at different excitation wavelengths without water's Raman signal. Intensity of QDs decreases significantly for all excitation wavelengths with respect to temperature. In figure 4, for the excitation wavelength of 310 nm (figure 4(a)), red shift of PL spectrum with respect to temperature can be found. Similar trend is observed for other wavelengths (figures 4(b) and (c)). In addition, as wavelength becomes longer, the excited fluorescence intensity become weaker. It reveals that when using fluorescence thermometry, shorter wavelength could give sound fluorescence signal and is more desirable for use in the measurement. Figure 5(a)

presents the temperature dependence of PL intensity for different excitation wavelengths. PL intensities are normalized by the intensity at the lowest temperature. There is around 50% decrease for the little temperature range of 75 °C, which is very significant comparing with other traditional semiconductor QDs (e.g. about 5.8% drop for the temperature difference of 19.2 °C in refs. 20) [19, 20, 24]. The physics behind this phenomenon can be understood as follows: PL intensity of QDs can be obtained from $F_l = \Phi \cdot I \cdot B$, where product of $I \cdot B$ is the absorption of light, Φ is quantum efficiency (or called quantum yield) of photon excitation. The quantum efficiency involves both radiative decay and non-radiative decay of excited states as: $\Phi = \Gamma_r / (\Gamma_r + \Gamma_{nr})$, where Γ_r is radiative decay rate and Γ_{nr} is non-radiative decay rate. Usually, the radiative decay rate is not affected by temperature but non-radiative decay rate is temperature dependent by the Boltzmann distribution as: $A \cdot \exp(-E/kT)$, where A is a constant, E is state energy, k is the Boltzmann's constant and T is the thermodynamic temperature. As temperature increases, the non-radiative decay rate increases, thus the quantum efficiency decreases as well as the corresponding PL intensity. In addition, it shows that the temperature coefficients of normalized intensity for different wavelengths are the same, which means that it can be used for different excitation wavelength if its photon energy is strong enough to excite sound fluorescence signals.

The red shift (Stokes shift) of PL signal is another common feature for many QDs, which is also resulted from the non-radiative decay to the lowest vibrational energy level of the excited state. When the temperature is increased, thermally induced volumetric displacement (equilibrium spacing

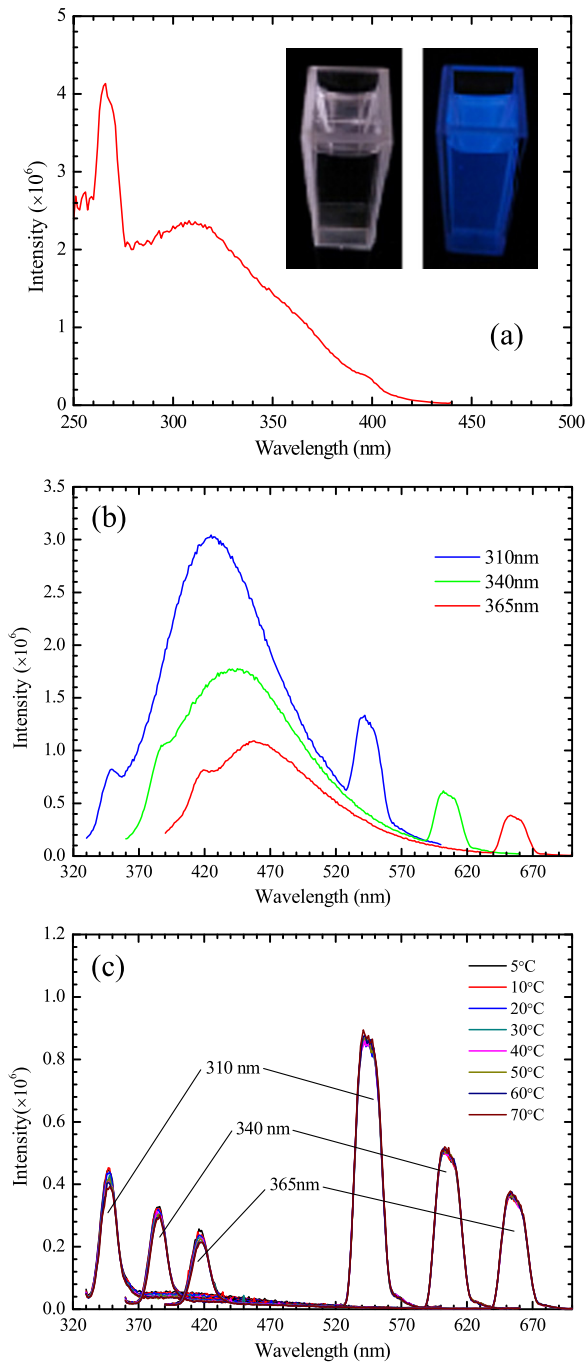


Figure 3. Characterization of GQDs aqueous solution. (a) Absorption spectrum of GQDs solution with detection wavelength of 460 nm shows two absorption bands at about 265 nm and 310 nm. Inserts are the photos of GQDs solution under visible light (left) and a UV lamp (right). (b) PL spectrum of the GQDs at different excitation wavelengths at room temperature (20 °C). With excitation wavelength varies from 310 to 365 nm, the PL peak shifts from 425 to 458 nm. (c) Emission spectrum of the distilled water at different temperature under 310 nm, 340 nm and 365 nm excitation wavelength to examine that water's emission spectrum has rare temperature-dependence at different excitation wavelengths.

of atoms) of the lattice could affect phonon energy exchange during fluorescence excitation which thus changes the photon energy of the excited fluorescence signal. This can be somewhat explained by the temperature dependence of

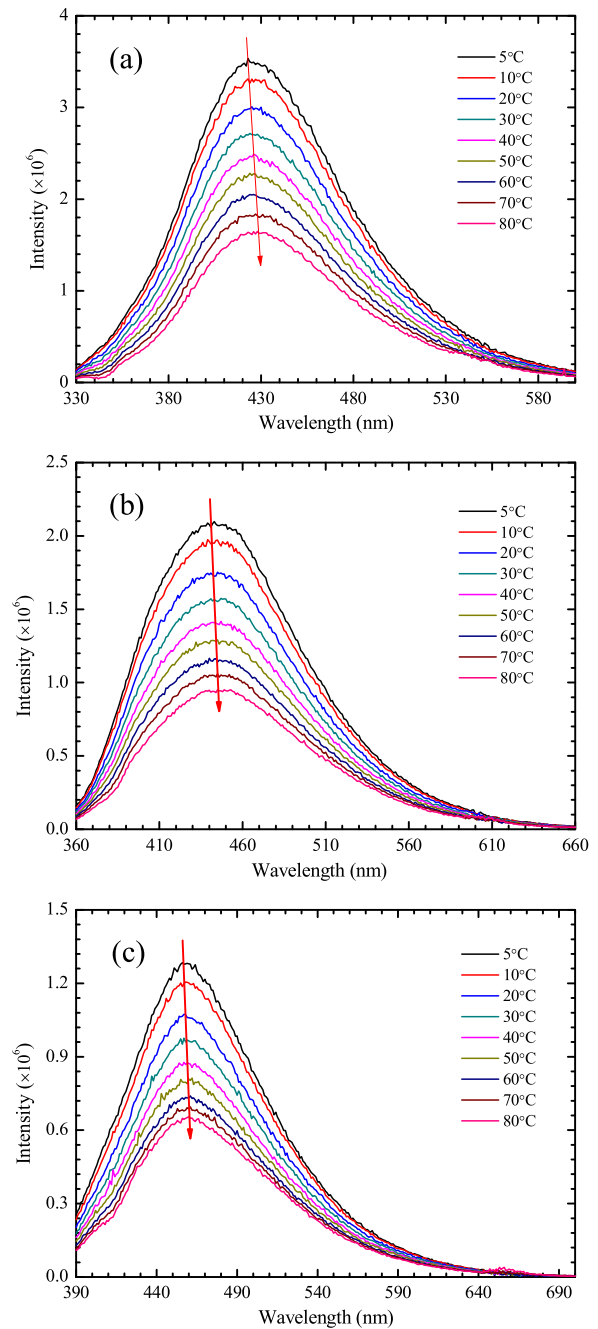


Figure 4. PL spectrum of the GQDs in different temperature at 310 nm (a), 340 nm (b) and 365 nm (c) excitation wavelength after removing water signal. The PL spectrum has a red-shift and its intensity decreases with respect to the temperature for all excitation wavelengths.

energy gap of semiconductors as $E(T) = E_0 + \sum_i A_i [2n_{BE}(E_i/k_B T) + 1]$, where A_i are the weights, n_{BE} is Bose–Einstein factor. For GQDs, the fluorescence spectrum of GQDs is broad and the red shifts phenomenon is not apparent. Therefore, the commonly used method either Gaussian or Lorentz fitting to get peak position is not applicable. We define the value on x-axis of a 1/2 integration area of the peak as the ‘theoretical’ peak position to distinguish the red shift. By using this method, the slight change in fluorescence frequency can be distinguished as

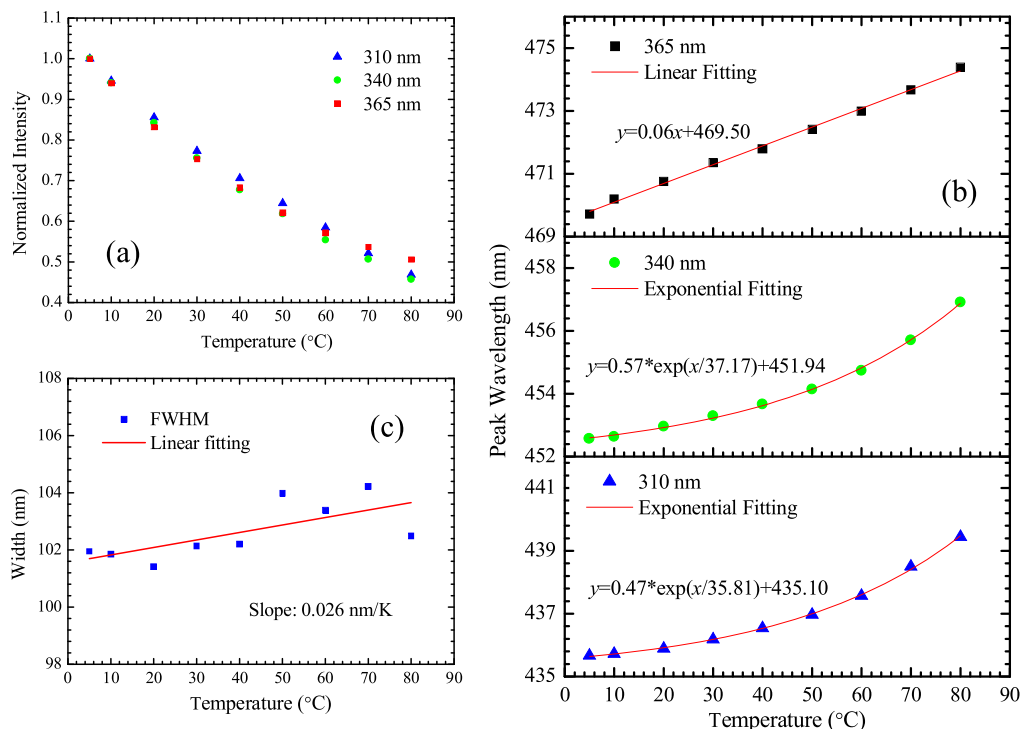


Figure 5. (a) Temperature-dependence of normalized PL spectrum intensity from 5 to 80 °C. The similar trend in the significantly decreased intensity (more than 50%) for the temperature range of 75 °C for all the excitation wavelengths validates that PL intensity of GQDs is an effective temperature sensor which can be applied under various excitation conditions. (b) Peak position as a function of temperature for different wavelengths. The peak shifts are 3.78 nm, 4.34 nm and 4.67 nm for wavelengths of 310 nm, 340 nm and 365 nm respectively. (c) The FWHM as a function of temperature linearly with coefficient of 0.026 nm K⁻¹. The signal is not as significant as either normalized intensity or peak shift.

shown in figure 5(b). It is found that all the spectrum peak shifts to the longer wavelengths with different trend with temperature. For the excitation wavelength of 310 nm and 340 nm, the peak position has an apparently exponential relationship with temperature as $y = 0.47 \times \exp(x/35.81) + 435.1$ and $y = 0.57 \times \exp(x/37.17) + 451.94$ respectively. For the excitation wavelength of 365 nm, the peak position shows a more like linear relationship with temperature as: $y = 0.062x + 469.5$. Figure 5(b) shows that the temperature coefficient has a close relation with the excitation wavelength. For our sample with current control conditions, the peak shift for longer excitation wavelengths has larger temperature coefficient. The peak shifts for wavelengths of 310 nm, 340 nm and 365 nm are 3.78 nm, 4.34 nm and 4.67 nm with temperature increases from 5 to 80 °C. The relatively larger peak shifts for longer wavelengths than short wavelength for our sample reveal that the temperature calibration using longer wavelengths is more accurate than using lower wavelengths in thermal applications. However, it is also limited by the gradually decreased fluorescence spectrum as excitation wavelength increases and deviates from the absorption band. In addition, only temperature is considered in this experiment to distinguish the effect of wavelength. If other experimental conditions, for example, pH value or dimension of GQDs are considered, the wavelength dependence of temperature coefficient of peak shift might be more complicated.

It is observed from our results that one temperature shows good linear relationship while the other two are not. Usually the peak shift should be in linear relationship with this small temperature range as experimentally validated by many studies of other quantum dots [17–21]. The difference of our result with others comes from the curve fitting in our data processing. For our fluorescence spectra, the linewidth of the peak is broad and the peak is not very symmetric. This could be the reason for our observed nonlinear relationship between wavelength and temperature for these two temperatures. These curves can be used for temperature calibration, and are only applicable for temperature measurement as long as the data processing in the measurement experiment uses the same method. This method is very effective to distinguish small peak shift or within small temperature range since very little uncertainties are involved in the data processing.

Another feature for the temperature dependence of fluorescence spectrum is the peak width, which defined as the full width at half maximum (FWHM). In our work, the FWHM is defined as the width between points of the curve when PL intensity drops to the half of the peak intensity. It is observed from the longest wavelength of 365 nm (as shown in figure 5(c)) that FWHM has slight linear relationship with temperature but with high uncertainties. Therefore, this feature is not significant with temperature sensitivity ~ 0.026 nm K⁻¹, which is about half of peak shift. Such trend is not shown in two other wavelength due to the low sensitivity and high uncertainty in data processing. Compared with

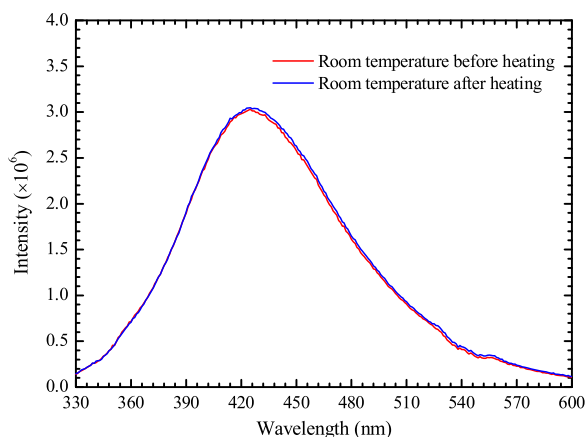


Figure 6. The PL spectrum at room temperature before (red solid line) and after heating (blue solid line) at 310 nm excitation wavelength. Several repeats for the heating and cooling experiments were performed and nearly identical spectrum indicates that PL of GQDs has a good stability and reversibility during thermal measurement.

peak intensity and shift features, the sensitivity of peak width is not as good as the other two, but it still a good reference for temperature probing if the fluorescence peak is narrow and peak width can be accurately determined.

For the implementations of GQDs into thermal applications, it requires the fluorescence spectroscopy of GQDs behaving good stability and reversibility before/after temperature rise. To validate this characteristic, the spectroscopy of GQDs is first recorded at room temperature and recorded again after heating sample to 80 °C (keep for one hour) then cooling it down to room temperature. This experiment was repeated for several times on the same batch of the sample. Figure 6 shows that the fluoroscopy spectra at room temperature before (red solid line) and after (blue solid line) heating experiment is almost the same, indicating that fluorescence spectroscopy of GQDs has a good stability and reversibility, and could be even better than other semiconductor QDs [24]. In addition, although semiconductor QDs have been demonstrated to be good temperature indicators [20, 21], some of them are intrinsic toxic [25–27] which limit the implementation in many biology applications [28, 29]. GQDs exhibit superior biocompatibility and extremely low cytotoxicity and have great potentials in the field of bio-imaging and bio-sensing with their excellent fluorescence emission characteristics [5, 30]. The combination of excellent compatibility and good temperature dependence would make fluorescence spectroscopy of GQDs an excellent candidate for bio-thermal imaging as well as other industrial applications.

4. Conclusion

Temperature dependence of fluorescence spectroscopy of GQDs was thoroughly investigated in this work. The PL intensity features most significant temperature response with normalized intensity decreases about 50% as temperature increases from 5 °C to 80 °C for the wavelengths of 310 nm,

340 nm and 365 nm. The peak shift feature also has a strong temperature-dependence with temperature coefficients larger than 0.050 nm K⁻¹ at these wavelengths. Not as such significant response is observed for the peak width (FWHM) feature which is caused by the low sensitivity and the large uncertainty in data processing because the PL curve is broad. Combined with stability and reversibility analysis during temperature increase, fluorescence spectroscopy of GQDs has been demonstrated be very effective in temperature probing for broad applications including bio-thermal field.

Acknowledgements

The financial supports from National Science Foundation of China (No. 51206124) and SRF for ROCS, SEM are gratefully acknowledged.

References

- [1] Geim A K 2009 Graphene: status and prospects *Science* **324** 1530–4
- [2] Li L-S and Yan X 2010 Colloidal graphene quantum dots *J. Phys. Chem. Lett.* **1** 2572–6
- [3] Kim S *et al* 2012 Anomalous behaviors of visible luminescence from graphene quantum dots: interplay between size and shape *ACS Nano* **6** 8203–8
- [4] Pan D *et al* 2012 Cutting sp²clusters in graphene sheets into colloidal graphene quantum dots with strong green fluorescence *J. Mater. Chem.* **22** 3314–8
- [5] Zhu S *et al* 2011 Strongly green-photoluminescent graphene quantum dots for bioimaging applications *Chem. Commun.* **47** 6858–60
- [6] Zhang L, Xing Y, He N, Zhang Y, Lu Z, Zhang J and Zhang Z 2012 Preparation of graphene quantum dots for bioimaging application *J. Nanosci. Nanotechnology* **12** 2924–8
- [7] Guo C X, Yang H B, Sheng Z M, Lu Z S, Song Q L and Li C M 2010 Layered graphene/quantum dots for photovoltaic devices *Angew. Chem., Int. Ed.* **49** 3014–7
- [8] Yan X, Cui X, Li B and Li L-S 2010 Large, solution-processable graphene quantum dots as light absorbers for photovoltaics *Nano Lett.* **10** 1869–73
- [9] Gupta V, Chaudhary N, Srivastava R, Sharma G D, Bhardwaj R and Chand S 2011 Luminescent graphene quantum dots for organic photovoltaic devices *J. Am. Chem. Soc.* **133** 9960–3
- [10] Shen J, Zhu Y, Yang X, Zong J, Zhang J and Li C 2012 One-pot hydrothermal synthesis of graphene quantum dots surface-passivated by polyethylene glycol and their photoelectric conversion under near-infrared light *New J. Chem.* **36** 97–101
- [11] Li Y, Hu Y, Zhao Y, Shi G, Deng L, Hou Y and Qu L 2011 An electrochemical avenue to green-luminescent graphene quantum dots as potential electron-acceptors for photovoltaics *Adv. Mater.* **23** 776–80
- [12] Ran X, Sun H, Pu F, Ren J and Qu X 2013 Ag nanoparticle-decorated graphene quantum dots for label-free, rapid and sensitive detection of Ag⁺ and biothiols *Chem. Commun.* **49** 1079–81
- [13] Pan D, Zhang J, Li Z and Wu M 2010 Hydrothermal route for cutting graphene sheets into blue-luminescent graphene quantum dots *Adv. Mater.* **22** 734–8

- [14] Bao L, Zhang Z L, Tian Z Q, Zhang L, Liu C, Lin Y, Qi B and Pang D W 2011 Electrochemical tuning of luminescent carbon nanodots: from preparation to luminescence mechanism *Adv. Mater.* **23** 5801–6
- [15] Tang L, Ji R, Cao X, Lin J, Jiang H, Li X, Teng K S, Luk C M, Zeng S and Hao J 2012 Deep ultraviolet photoluminescence of water-soluble self-passivated graphene quantum dots *ACS Nano* **6** 5102–10
- [16] Yue Y and Wang X 2012 Nanoscale thermal probing *Nano. Rev.* **3** 11586
- [17] Dai Y, Fan J, Chen Y, Lin R, Lee S and Lin H 1997 Temperature dependence of photoluminescence spectra in InAs/GaAs quantum dot superlattices with large thicknesses *J. Appl. Phys.* **82** 4489–92
- [18] Walker G W, Sundar V C, Rudzinski C M, Wun A W, Bawendi M G and Nocera D G 2003 Quantum-dot optical temperature probes *Appl. Phys. Lett.* **83** 3555–7
- [19] Al Salman A, Tortschanoff A, Mohamed M, Tonti D, Van Mourik F and Chergui M 2007 Temperature effects on the spectral properties of colloidal CdSe nanodots, nanorods, and tetrapods *Appl. Phys. Lett.* **90** 093104
- [20] Li S, Zhang K, Yang J-M, Lin L and Yang H 2007 Single quantum dots as local temperature markers *Nano Lett.* **7** 3102–5
- [21] Gu P, Zhang Y, Feng Y, Zhang T, Chu H, Cui T, Wang Y, Zhao J and William W Y 2013 Real-time and on-chip surface temperature sensing of GaN LED chips using PbSe quantum dots *Nanoscale* **5** 10481–6
- [22] Shen J, Zhu Y, Yang X and Li C 2012 Graphene quantum dots: emergent nanolights for bioimaging, sensors, catalysis and photovoltaic devices *Chem. Commun.* **48** 3686–99
- [23] Liu R, Wu D, Feng X and Müllen K 2011 Bottom-up fabrication of photoluminescent graphene quantum dots with uniform morphology *J. Am. Chem. Soc.* **133** 15221–3
- [24] Dai Q, Zhang Y, Wang Y, Hu M Z, Zou B, Wang Y and Yu W W 2010 Size-dependent temperature effects on PbSe nanocrystals *Langmuir* **26** 11435–40
- [25] Derfus A M, Chan W C and Bhatia S N 2004 Probing the cytotoxicity of semiconductor quantum dots *Nano Lett.* **4** 11–8
- [26] Lovrić J, Bazzi H S, Cuie Y, Fortin G R, Winnik F M and Maysinger D 2005 Differences in subcellular distribution and toxicity of green and red emitting CdTe quantum dots *J. Mol. Med.* **83** 377–85
- [27] Hardman R 2006 A toxicologic review of quantum dots: toxicity depends on physicochemical and environmental factors *Environ. Health Perspect.* **114** 165–72
- [28] Michalet X, Pinaud F F, Bentolila L A, Tsay J M, Doose S, Li J J, Sundaresan G, Wu A M, Gambhir S S and Weiss S 2005 Quantum dots for live cells, *in vivo* imaging, and diagnostics *Science* **307** 538–44
- [29] Hoshino A, Fujioka K, Oku T, Suga M, Sasaki Y F, Ohta T, Yasuhara M, Suzuki K and Yamamoto K 2004 Physicochemical properties and cellular toxicity of nanocrystal quantum dots depend on their surface modification *Nano Lett.* **4** 2163–9
- [30] Zhao H, Chang Y, Liu M, Gao S, Yu H and Quan X 2013 A universal immunosensing strategy based on regulation of the interaction between graphene and graphene quantum dots *Chem. Commun.* **49** 234–6